

## Electronic structure of rare-earth hydrides: $\text{LaH}_2$ and $\text{LaH}_3$

Michèle Gupta

*Le Centre de Mécanique Ondulatoire Appliquée du Centre National de la Recherche Scientifique 23, rue du Maroc-75019 Paris, France  
and la Faculté des Sciences d'Orsay, Bâtiment 510, 91405 Orsay, France\**

J. P. Burger

*Laboratoire de Physique des Solides, Bâtiment 510, Université Paris Sud, 91405 Orsay, France*

(Received 17 March 1980)

The electronic structure of the cubic stoichiometric hydrides  $\text{LaH}_2$  and  $\text{LaH}_3$  has been studied using the augmented-plane-wave method. The two low-lying hydrogen-metal bands of  $\text{LaH}_2$ , observed also for the fluorite structure transition-metal dihydrides, do not overlap the metal  $d$  bands; the Fermi energy  $E_F$  falls at the bottom of the rare-earth  $5d$  states and the density of states at  $E_F$  is lower than that of the pure metal. These results are analyzed in light of the resistivity, heat capacity, magnetic susceptibility, and NMR data; they can be schematically described in terms of a depopulation of the metal  $d$  bands upon formation of the dihydride. The Fermi-surface geometry of  $\text{LaH}_2$  is also studied and an evaluation of the electronic contribution to the electron-phonon coupling constant is performed by means of a simple model; the magnitude of this term is found to be small and we conclude that  $\text{LaH}_2$  should not be a superconductor, in agreement with existing data. In the trihydride, a third band appears at the low-energy side; the first three bands being separated by a gap of 0.53 eV from the metal  $d$  bands,  $\text{LaH}_3$  is found to be a semiconductor in agreement with resistivity measurements. The virtues of some aspects of the anionic model are discussed but the limits of this model are clearly assessed by means of a site and angular momentum analysis of the density of states which shows the hybridization of the low-lying bands; a comparison with x-ray-emission and photoelectron-spectroscopy data is also given.

### I. INTRODUCTION

The technological importance of the behavior of hydrogen in metals particularly for hydrogen-storage devices, hydrogen embrittlement, and catalysis, has motivated numerous experimental studies on transition and rare-earth-metal hydrides.<sup>1</sup> The lanthanides ( $L$ ) are known to have a good affinity for hydrogen; under certain conditions of temperature and pressure they form solid solutions ( $\alpha$  phase) and also compounds with a wide range of hydrogen concentrations, which are based upon the stoichiometric  $LH_2$  composition and can even reach (except for the divalent Eu and Yb) the  $LH_3$  composition.<sup>1</sup> The rare-earth dihydrides have the fluorite structure (except for  $\text{EuH}_2$  and  $\text{YbH}_2$  which are orthorhombic), the tetrahedral interstices of the fcc  $L$  lattice being occupied by the hydrogens. The trihydrides of the early members of the series (La through Nd) are cubic, and the additional hydrogen atoms fill the octahedral interstices; a contraction of the lattice is also observed from  $LH_2$  to  $LH_3$ . For the trihydrides or slightly substoichiometric compounds of the heavier lanthanides (Sm through Lu with the above-mentioned exceptions of Eu and Yb), the structure changes to hexagonal. Since the pioneering work of Switendick,<sup>2</sup> most of the theoretical effort has rather been focused on the transition-metal hydrides, while theoretical studies of the electronic structure of  $L$  hydrides remain scarce.<sup>3,4,5</sup> Thus, most of the numerous experiments which include resistivity,<sup>6-8</sup> heat capacity,<sup>9</sup>

magnetic susceptibility,<sup>10,11</sup> NMR data,<sup>12-14</sup> etc., have often been interpreted in terms of the simple  $\text{H}^-$  model, with the exception of some of them which, like the NMR data, are compatible with both the anionic and the protonic models. With the aim of interpreting some of the experimental data in terms of a more realistic picture of the electronic structure we have performed an *ab initio* augmented-plane-wave (APW) band-structure calculation for  $\text{LaH}_2$  and  $\text{LaH}_3$ . Although the defect structure plays an important role, we will be concerned here only with stoichiometric compounds. The remainder of this paper is organized as follows. In Sec. II the energy bands and density of states (DOS) of both hydrides are described with an emphasis on the change in the electronic structure of the pure rare-earth metal upon hydrogenation. Section III is devoted to an interpretation of the present results which can account for the drastic decrease in the magnetic susceptibility and heat capacity from the pure metal to the dihydride, as well as for the larger conductivity of the dihydride; the metal-insulator transition occurring between the  $\text{LaH}_2$  and  $\text{LaH}_3$  compositions is discussed. The apparent depopulation of the metal  $5d$  bands upon formation of the hydrides and some of the virtues of the anionic model are outlined; however, the site and angular momentum analysis of the DOS presented in Sec. IV shows clearly that the low-lying bands are not formed exclusively of hydrogen states and this indicates the limits of the anionic model. The partial DOS analysis is also discussed

in this section in light of x-ray emission experiments<sup>15</sup> and photoelectron spectroscopy data on dihydrides.<sup>16</sup> In Sec. V the band-structure results of  $\text{LaH}_2$  are used to evaluate the electronic term of the electron-phonon coupling constant  $\lambda$  using the model of Gaspari and Gyorffy<sup>17</sup>; the electronic contribution to  $\lambda$  arising from the hydrogen sites is extremely small and we find that  $\text{LaH}_2$  should not be a superconductor. This is in agreement with the data of Merriam and Schreiber<sup>18</sup> who showed that  $\text{LaH}_{1.96}$  is not superconducting down to 0.33 K.

## II. ENERGY BANDS AND DOS

As in our previous studies<sup>4,19</sup> of the fluorite-structure transition and rare-earth-metal dihydrides we have performed an ab initio calculation of the energy eigenvalues of  $\text{LaH}_2$  and  $\text{LaH}_3$  at 89 points in the  $\frac{1}{48}$ th irreducible fcc Brillouin zone (BZ) using the nonrelativistic APW method<sup>20</sup> with a warped muffin-tin potential in the interstitial region, to account for the deviations from a constant value, and treating the exchange term within the Slater local-exchange approximation. We used the  $5d^16s^2$  electronic configuration for La to obtain self-consistent atomic charge density. The choice of this configuration was guided by our previous experience in other transition and rare-earth-metal hydrides<sup>4,19</sup> and comparison with experimental data. We also note that for pure rare-earth metals, the choice of different configuration produces only a small change in the band structure<sup>21</sup> and does not affect the essential features or the

conclusions drawn.

For  $\text{LaH}_3$ , the tetrahedral and octahedral hydrogen muffin-tin spheres need to be treated as different species, since the sites are inequivalent, thus we did not use the simplifying assumption of Switendick for trihydrides<sup>3</sup> which consisted of taking identical potentials for the hydrogen atoms located at the tetrahedral and at the octahedral inequivalent sites. The APW wave functions were expanded in a variable set of reciprocal-lattice vectors to obtain a full convergence for each  $\vec{k}$  point. The DOS was then obtained by means of an accurate BZ integration scheme<sup>22</sup> involving the partition of the irreducible  $\frac{1}{48}$ th wedge of the BZ into 6144 microtetrahedra and a linear energy-eigenvalue interpolation scheme inside these microzones. The resulting energy bands and DOS are plotted, respectively, in Figs. 1 and 2 for  $\text{LaH}_2$  and Figs. 3 and 4 for  $\text{LaH}_3$ .

### A. $\text{LaH}_2$

For  $\text{LaH}_2$ , and as previously observed for other fluorite-structure metal dihydrides,<sup>2-4,19</sup> two bands are found at the low-energy side of Fig. 1. In Table I we give a decomposition of the charge at some high-symmetry points into its angular-momentum components (up to  $l=3$ ) inside the muffin-tin metal and hydrogen spheres. The lowest  $\Gamma_1$  point is a metal- $s$ -hydrogen- $s$  bonding state, while  $\Gamma'_2$  is formed by an antibonding combination of the two hydrogen  $s$  states in the unit cell. A residual metal  $f$  ( $l=3$ ) component is also found at  $\Gamma'_2$ .

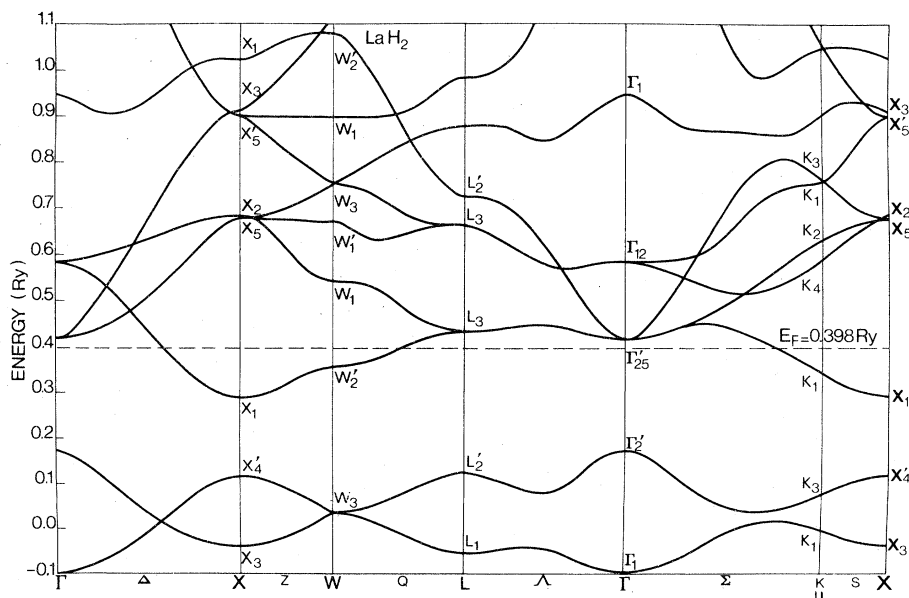


FIG. 1. Energy bands of  $\text{LaH}_2$  ( $a = 10.7128$  a.u.) along several symmetry directions of the fcc Brillouin zone. Energies are in rydberg.

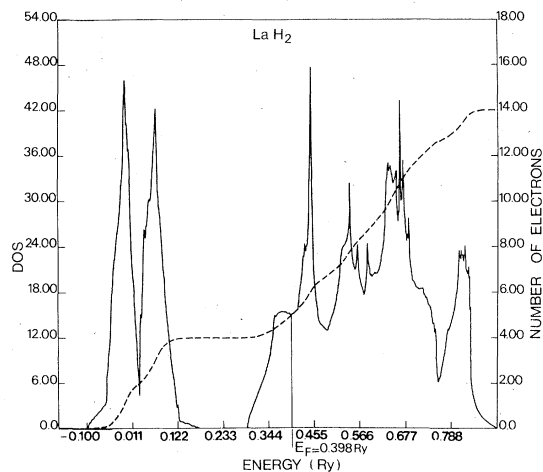


FIG. 2. Total density of states of  $\text{LaH}_2$  (full-line curve and left-hand side scale) units are states of both spin/Ry unit cell. The number of electrons (dashed-line curve and right-hand side scale).

The first two bands of total width 0.271 Ry are separated by an indirect gap of 0.118 Ry (between  $\Gamma'_2$  and  $X_1$ ) from the next band complex. The analysis presented in Table I shows that above the gap, the states have essentially a metal  $d$  character; at  $\Gamma$ , the fivefold degenerate metal  $d$  states are split by 0.167 Ry by the cubic field into a triply degenerate  $\Gamma'_{25}$  and doubly degenerate  $\Gamma'_{12}$  state. It is to be noted that, although the presence of the two low-lying metal-hydrogen bands is a feature common to all the fluorite-structure metal dihydrides,<sup>2-5</sup> the position and width of these bands depend sensitively upon both the metal-hydrogen distance and the

spatial extension of the metal  $d$  orbitals. As an example, for  $\text{TiH}_2$  which has a much smaller lattice constant ( $a=8.4260$  a.u.) compared to  $a=10.7128$  a.u. for  $\text{LaH}_2$ , we previously found<sup>19</sup> that the low-lying bands are much wider (0.75 Ry) and we obtained an overlap with the metal  $d$  states. On the contrary, for the rare-earth dihydrides  $\text{ErH}_2$  and  $\text{TbH}_2$  we observed,<sup>4</sup> as for  $\text{LaH}_2$ , a gap between the two low-lying bands and the metal  $d$  bands. As it can be seen in Fig. 2, two large peaks are found in the DOS of the first two bands of  $\text{LaH}_2$ . The first peak centered at  $E=-0.005$  Ry is due to flat bands around  $K_1$ ,  $X_3$ , and  $L_1$  while the second high peak centered at  $E=0.071$  Ry can be attributed to flat portions of the bands around  $W_3$  and along the  $\Sigma_3$  branch joining  $\Gamma'_2$  to  $K_3$ . The low-lying bands are filled by four of the five valence electrons of  $\text{LaH}_2$ ; the remaining electron fills the bottom of the metal  $5d$  bands. Thus the dihydride is metallic, in agreement with resistivity measurements.<sup>6-8</sup> The Fermi level falls only at 0.106 Ry above the bottom of the metal  $5d$  bands, and the DOS at the Fermi energy  $E_F$  is rather low:  $N(E_F)=15.05$  states of both spin/Ry unit cell. The shoulder in the DOS observed above  $E=0.34$  Ry corresponds to flat bands around  $W'_2$  and  $K_1$  in this energy range. The next sharp peak at  $E=0.447$  Ry arises mostly from the flat degenerate band joining  $\Gamma'_{25}$  to  $L_3$  in the  $\Delta$  direction, and would correspond to the filling of the bands by six electrons by a rigid shift of the Fermi energy. This important feature in the DOS of the metal bands has also been found by an ab initio calculation of the ideal stoichiometric compound of group IVB:  $\text{TiH}_2$ . For this compound, the Fermi

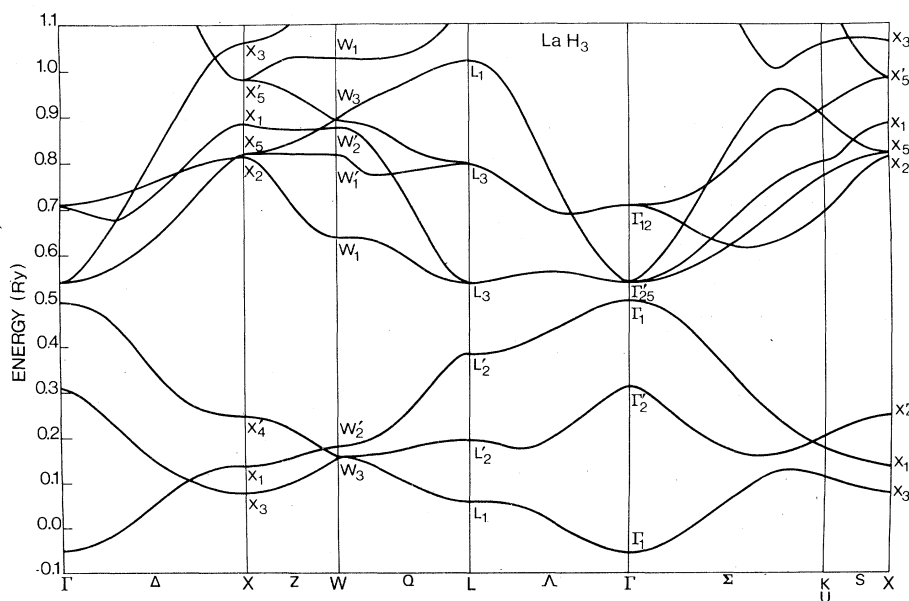


FIG. 3. Energy bands of  $\text{LaH}_3$  ( $a=10.5864$  a.u.) along several high-symmetry directions. Energies are in rydberg.

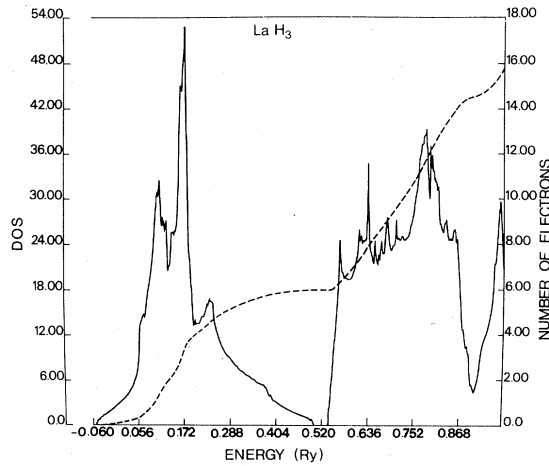


FIG. 4. Total density of states of LaH<sub>3</sub> (full-line curve and left-hand side scale) units are states of both spin/Ry unit cell. The number of electrons (dashed-line curve and right-hand side scale).

energy falls in the peak of the DOS which also arises from a degenerate flat band in the  $\Lambda$  direction. This structure has led to interpret the tetragonal distortion of group IVB dihydrides TiH<sub>2</sub> and ZrH<sub>2</sub> in terms of a Jahn-Teller-type effect<sup>23,2,19</sup>

which lifts the degeneracy of the flat band in the  $\Lambda$  direction. It is remarkable that the peak in the DOS due to this flat band is also present in the case of the trivalent rare-earth dihydrides. We also have observed it<sup>4</sup> for ErH<sub>2</sub> and TbH<sub>2</sub>. The similar flat degenerate  $\Gamma'_{25}L_3$  band is also present in the recent band calculation<sup>24</sup> of trivalent transition-metal dihydrides YH<sub>2</sub> and ScH<sub>2</sub>. Such structure in the  $d$  bands is remarkably insensitive to the detail of the potential which differs with the compound under study and suggests that a rigid-band model applied to the  $d$  bands of one of the early transition or rare-earth dihydrides can be good enough to obtain qualitative information for other dihydrides at the Fermi energy. On the contrary, the width and position of the low-lying bands depend quite sensitively upon the compound under study.

The Fermi surface (FS) of LaH<sub>2</sub> is much simpler than that of the pure metal since it is formed only by one band (band 3) at the bottom of the metal  $5d$  states, as it can be seen in Fig. 1. The FS cross sections by two high-symmetry planes are shown in Fig. 5. The FS of LaH<sub>2</sub> is a multiply connected hole surface formed of a warped cube around  $\Gamma$  with necks along the  $\Gamma L$  directions. Similar geometry has been obtained for the FS of other rare-

TABLE I. Site and angular momentum analysis of the charge for some high-symmetry points. The charge corresponding to each normalized wave function is analyzed inside the muffin-tin La and H spheres ( $R_{\text{MT}}^{\text{La}} = 2.8577$  a.u. and  $R_{\text{MT}}^{\text{H}} = 1.7333$  a.u.).

$\vec{k}$	Energy (Ry)	La site				2H sites			
		$s$	$p$	$d$	$f$	$s$	$p$	$d$	$f$
$\Gamma_1$	-0.097	0.1190	0.0	0.0	0.0	0.4989	0.0	0.0	0.0
$\Gamma'_2$	0.174	0.0	0.0	0.0	0.0134	0.8125	0.0	0.0	0.0
$\Gamma'_{25}$	0.417	0.0	0.0	0.5865	0.0	0.0	0.0883	0.0018	0.0
$\Gamma_{12}$	0.584	0.0	0.0	0.7297	0.0	0.0	0.0	0.0124	0.0
$X_3$	-0.037	0.0	0.0	0.2027	0.0	0.5400	0.0	0.0015	0.0003
$X'_4$	0.119	0.0	0.1363	0.0	0.0027	0.6321	0.0	0.0003	0.0001
$X_1$	0.292	0.0245	0.0	0.3618	0.0	0.0	0.0452	0.0036	0.0
$X_5$	0.676	0.0	0.0	0.8097	0.0	0.0	0.0404	0.0105	0.0021
$X_2$	0.685	0.0	0.0	0.8148	0.0	0.0	0.0	0.0	0.0041
$W_3$	0.036	0.0	0.0631	0.1293	0.0011	0.5672	0.0005	0.0014	0.0002
$W'_2$	0.357	0.0	0.0292	0.3866	0.0002	0.0	0.0349	0.0053	0.0004
$W_1$	0.541	0.0378	0.0	0.5034	0.0155	0.0	0.0471	0.0010	0.0016
$W'_1$	0.673	0.0	0.0	0.8144	0.0	0.0	0.0403	0.0107	0.0020
$W_3$	0.754	0.0	0.0396	0.5770	0.0151	0.1005	0.0491	0.0068	0.0015
$K_1$	-0.004	0.0037	0.0297	0.1657	0.0005	0.5468	0.0009	0.0014	0.0002
$K_3$	0.077	0.0	0.0966	0.0738	0.0019	0.5960	0.0004	0.0009	0.0002
$K_1$	0.342	0.0101	0.0202	0.3780	0.0002	0.0024	0.0400	0.0043	0.0003
$K_4$	0.587	0.0	0.0152	0.6284	0.0077	0.0	0.0244	0.0026	0.0020
$K_2$	0.630	0.0	0.0	0.7487	0.0067	0.0	0.0495	0.0098	0.0012
$K_1$	0.755	0.0	0.0159	0.7522	0.0027	0.0680	0.0311	0.0097	0.0024
$K_3$	0.762	0.0788	0.0401	0.2991	0.0304	0.0421	0.0928	0.0033	0.0011
$L_1$	-0.051	0.0362	0.0	0.1393	0.0	0.5324	0.0019	0.0002	0.0003
$L'_2$	0.125	0.0	0.1179	0.0	0.0040	0.6464	0.0009	0.0001	0.0001
$L_3$	0.434	0.0	0.0	0.5788	0.0	0.0	0.0583	0.0047	0.0001
$L_3$	0.665	0.0	0.0	0.8012	0.0	0.0	0.0110	0.0094	0.0015
$L'_2$	0.726	0.0	0.0586	0.0	0.0595	0.0837	0.0457	0.0044	0.0005

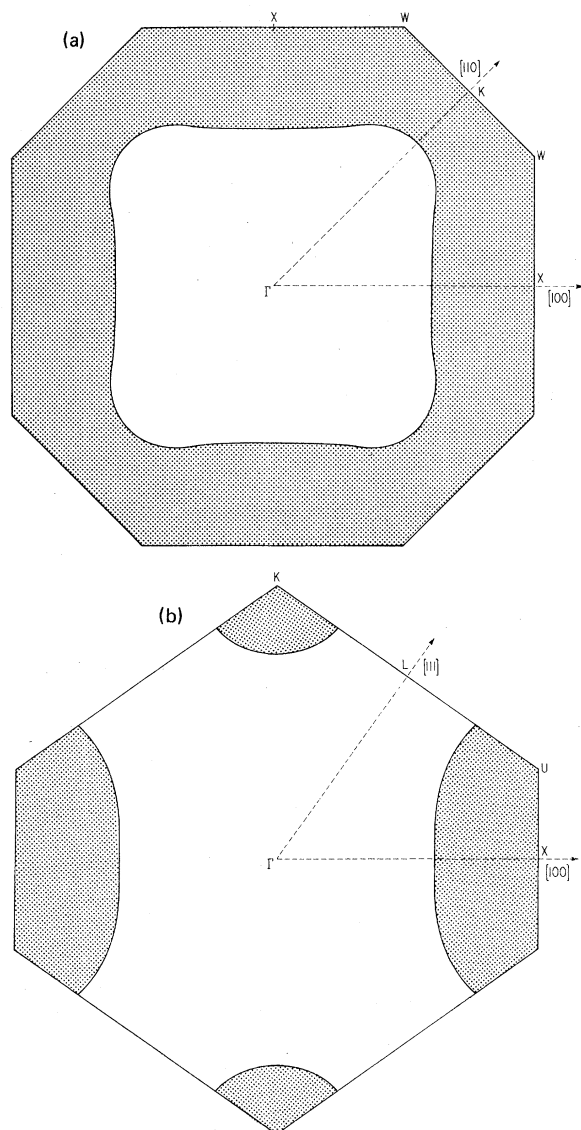


FIG. 5. Fermi-surface cross sections of  $\text{LaH}_2$  by two high-symmetry planes (a)  $\Gamma XW$ ; (b) plane  $\Gamma XL$ . The dotted portions are occupied regions.

earth-metal dihydrides<sup>4</sup>  $\text{ErH}_2$  and  $\text{TbH}_2$ , although the exact dimensions show a slight variation with the compound under study and could of course be somewhat modified by relativistic effects. However, since band 3 is not flat and shows a sizable dispersion, relativistic effects are not expected to modify drastically the geometry of this Fermi surface.

#### B. $\text{LaH}_3$

For the trihydride  $\text{LaH}_3$ , we can see in Fig. 3 that a third band appears at low energy, below the

metal  $d$  states, as was first obtained by Switendick<sup>2</sup> for  $\text{YH}_3$ . A wave-function analysis at  $\Gamma$  shows that the lowest  $\Gamma_1$  point is formed of bonding metal  $s$  and tetrahedral and octahedral hydrogen  $s$  states;  $\Gamma'_2$  is an antibonding combination mostly of the tetrahedral hydrogen  $s$  states like in the dihydride while the highest  $\Gamma_1$  point is an antibonding combination of metal- and tetrahedral hydrogen states with octahedral hydrogen  $s$  states. Such a band was, of course, not observed in the electronic structure of  $\text{LaH}_2$ . Because of the lattice contraction (the lattice constant of  $\text{LaH}_3$   $a = 10.5864$  a.u. is 1.2% smaller than that of  $\text{LaH}_2$ ), the lowest  $\Gamma_1$  point in  $\text{LaH}_3$  has a lower energy relative to the metal  $d$  states than in  $\text{LaH}_2$  while the antibonding  $\Gamma'_2$  state shows the reverse trend. This leads to an increase in the energy difference between  $\Gamma_1$  and  $\Gamma'_2$  from 0.271 Ry in  $\text{LaH}_2$  to 0.364 Ry in  $\text{LaH}_3$ . The total width of the metal-hydrogen low-lying states which is 0.551 Ry for  $\text{LaH}_3$  is much larger than in the dihydride due to the further increase provided by the additional band. In the DOS of  $\text{LaH}_3$  plotted in Fig. 4, several peaks are found; at  $E = 0.109$  Ry, the structure coincides with the crossing of the  $\Delta_1$  and  $\Delta'_2$  branches and with a flat branch around  $K_1$ . The next peak at  $E = 0.164$  Ry is due to flat branches around  $W_3$  and to the bottom of the  $\Sigma_3$  branch, while the highest peak at 0.175 Ry corresponds to the crossing of the  $Z_3$  and  $Z_1$  branches and to flat regions around  $W'_2$  as well as to the bottom of the  $\Lambda_1$  branch. The three low-lying bands are separated by an indirect gap of 38 mRy between  $\Gamma_1$  and  $L_3$  from the metal  $5d$  bands. The low-lying bands are filled by the six valence electrons of the trihydride and the results of the band-structure calculation can thus account for the observed semiconducting properties.<sup>6-8</sup> The value of the gap presently found for  $\text{LaH}_2$  is larger than the value of 0.104 eV obtained experimentally<sup>25</sup> for  $\text{CeH}_{2.81}$ ; part of the difference can be explained by the lattice contraction in the  $\text{LaH}_2$  series which is expected to raise the  $\Gamma_1$  high level. The  $d$  bands of  $\text{LaH}_3$  above the energy gap are somewhat different from those obtained for  $\text{LaH}_2$  since additional metal  $d$  states have been lowered by the metal-hydrogen interaction to form a third low-lying band. The crystal-field splitting of the  $5d$  states at  $\Gamma$  is, however, almost unchanged between the two compounds.

### III. INTERPRETATION

We wish to interpret the changes in the band structure upon increasing hydrogenation and explain some experimental data by means of the results described in Sec. II. If we compare the electronic structure of the pure rare-earth metal<sup>26</sup> to that of the dihydride and focus our attention on the

position of the Fermi level we can see that in the pure metal, the Fermi level lies much higher in energy from the bottom of the metal  $5d$  bands hybridized by the  $s$ - $p$  band than in the dihydride. As mentioned previously, the Fermi energy of the dihydride is rather found at the bottom of the metal  $5d$  bands. The DOS of the pure metal is consequently higher than in the dihydride for which we found 15.05 states of both spin/Ry unit cell; specific-heat data<sup>27</sup> give a DOS of 33.18 and 27.2 states of both spin/Ry-atom, respectively, for the fcc and the  $d$ -hcp phases of pure La. These values should of course be reduced by the electron-phonon enhancement factor prior to comparison to a band-structure DOS. The bare DOS of  $d$ -hcp La was found<sup>26</sup> to be 19.4 states of both spin/Ry atom. Thus, at first sight, the net result appears as a depopulation of the metal  $d$  bands upon hydrogenation. This qualitative remark explains the success of the anionic model often invoked to interpret numerous experiments on rare-earth hydrides in which the properties at the Fermi energy are sampled. However, we shall see in Sec. IV that this convenient simple picture should not be taken too literally and that the rigid-band model applied to the pure-metal bands is erroneous. The decrease in  $N(E_F)$  from the pure metal to the dihydride obtained in the present calculation is in agreement with magnetic susceptibility measurement<sup>10</sup>; for  $\text{LaH}_{2.03}$  the susceptibility  $X$  was found to be  $0.4 \times 10^{-6}$  emu/g, a value which is a factor of 2 smaller than that of the pure metal. Similarly, in his study of the nuclear magnetic resonance of La, Schreiber<sup>28</sup> found that the spin-lattice relaxation rate  $T_1$ , which is inversely proportional to  $N^2(E_F)$ , is 220 times larger in  $\text{LaH}_2$  than in pure La while the Knight shift of  $\text{LaH}_2$  is 0.33 that of La. Although the interpretation of these data is complex due to the lack of exact knowledge about the relative importance of the different contributions to the Knight shift (core-polarization effects, orbital contribution, and contact interaction), these experiments suggest a decrease of the DOS at  $E_F$  from the metal to the dihydride, in agreement with the present calculation. This trend is also corroborated by the electronic specific-heat measurements which<sup>9,27</sup> show a decrease from  $\gamma = 2.75 \pm 0.07$  mcal mole<sup>-2</sup> K<sup>-2</sup> for fcc La to  $\gamma = 2.041$  mcal mole<sup>-1</sup> K<sup>-2</sup> for  $\text{LaH}_{2.03}$ . The net depopulation of the metal  $d$  bands upon hydrogenation, which is also a feature common to the rare-earth dihydrides such as  $\text{ErH}_2$  and  $\text{TbH}_2$  having  $4f$  electrons,<sup>4</sup> plays an important role in the magnetic properties of these compounds. The Ruderman-Kittel-Kasuya-Yoshida<sup>29</sup> (RKKY) indirect-exchange interaction between the rare-earth ion magnetic moments transmitted by the polarization of the con-

duction electrons is expected to be weaker in the hydrides since there are fewer conduction electrons than in the pure rare-earth metals. This can explain why the ordering temperatures of the magnetic  $L$  hydrides are consistently lower than those of the pure  $L$  metals.<sup>30</sup>

As we have indicated in Sec. II, the band-structure results can account for the metallic properties of  $\text{LaH}_2$  and the semiconducting behavior of  $\text{LaH}_3$  in agreement with the experimental data.<sup>6-8</sup> Most of the earlier work on the resistivity of  $L$  hydrides has been performed by Daou<sup>9</sup> who showed that the resistivity of the dihydrides is always much smaller than that of the corresponding  $L$  metal, the reduction ratio ranging from 2 to 5 for the elements with magnetic moments; for  $\text{LaH}_2$  and  $\text{LuH}_2$  the reduction ratio is, respectively, 3 and 7. This feature could be due to the reduction of the electron scattering mechanism into  $d$  states since, as we mentioned previously, the Fermi level of the dihydride is located at the bottom of the  $5d$  metal band. Several experimental results show that the transition from metallic to semiconducting behavior upon increasing hydrogen content occurs before the hydrogen-to-metal ratio reaches the value  $x=3$ . The resistivity studies<sup>6-8</sup> reveal a drastic drop in the conductivity when  $x=2.8$ . The study of the magnetic resonance of the proton in  $\text{LaH}_x$  reveals<sup>31</sup> that while the product  $T_1 T$  for  $\text{LaH}_{2.08}$  has a value of  $74 \pm 5$  sec K typical of metallic conduction, the Korringa relation is not obeyed in the case of  $\text{LaH}_{2.80}$ ; rather,  $T_1$  follows a law typical of semiconductors. The magnetic susceptibility<sup>10</sup> which decreases from the pure metal to the dihydride continues to drop as  $x$  increases above the value of 2.0 to become zero for  $x \approx 2.7$  and negative for higher values of  $x$ . We wish to recall at this point that prior to the first band-structure calculations on hydrides,<sup>2</sup> both the anionic and the protonic models had been invoked to account for the metal-semiconductor transition. In the protonic model,<sup>32</sup> the electrons of the hydrogen atoms were assumed to fill the metal conduction bands, and the contraction of the lattice for hydrogen-to-metal ratios greater than 2 was assumed to result in a splitting of the  $5d$ - $6s$  metal band into two subbands, the lowest manifold being able to accommodate six electrons was therefore fully occupied by the six electrons of  $\text{LaH}_3$  and the semiconducting properties were thus explained. The present calculation however rules out the possibility of such a mechanism. Although, as we shall see later, the three low-lying bands found in the trihydride are not formed only of hydrogen states, the anionic model proposed by Libowitz<sup>25</sup> to explain the conductivity data seems to be closer to the reality. In this model, the vacancies of the substoichiometric

compounds  $2.8 < x < 3.0$  act as donors and the semiconductor should be of  $n$  type. Thermoelectric power measurements<sup>25</sup> on cerium hydrides for  $2.38 < x < 2.85$  show that indeed the Seebeck coefficient which is positive for the metallic compounds becomes strongly negative above the metal-to-semiconductor transition indicating a  $n$ -type semiconductivity. The hole-type conductivity of the metallic nonstoichiometric compounds which is revealed by the thermoelectric power measurements<sup>25</sup> and the Hall-effect studies<sup>32</sup> could be accounted for by the formation of a defect band, as proposed by Bos<sup>33</sup> and Libowitz<sup>25</sup> although these authors attribute a different origin to the defect band. Further speculations concerning theoretical models will have to wait for a study of the electronic structure of nonstoichiometric compounds. This could be done by means of the coherent-potential-approximation method which has already been used for other hydrides.

#### IV. PARTIAL DOS ANALYSIS AND COMPARISON WITH EXPERIMENTAL SPECTRA

In order to gain some insight on the composition of the band we show in Figs. 6 to 9 a decomposition of the DOS into its angular momentum components inside the metal and hydrogen muffin-tin (MT) spheres of  $\text{LaH}_2$ . The wave functions outside the MT spheres are not analyzed in this decomposition, since they cannot be assigned in a unique way to either of the MT spheres. It can be clearly seen that the two low-lying bands are largely formed by hydrogen  $s$  states. The shape of  $l=0$  component of the DOS inside the hydrogen spheres has the two-peak structure discussed previously, and its shape

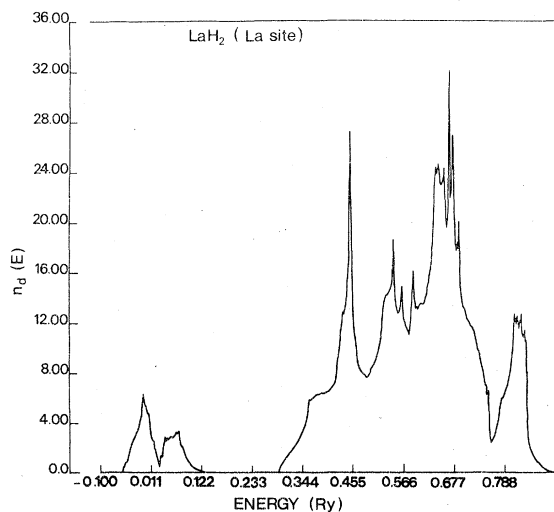


FIG. 6. Partial  $d$  ( $l=2$ ) DOS inside the muffin-tin La sphere. Units are states of both spin/Ry unit cell.

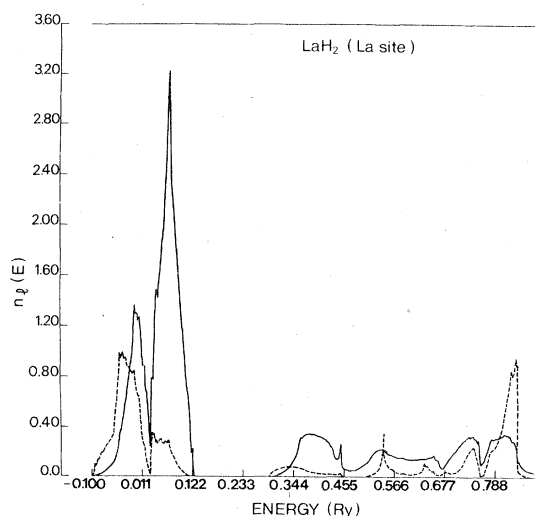


FIG. 7. Partial-wave analysis of the DOS inside the muffin-tin La sphere. Units are states of both spin/Ry unit cell. The  $s$  ( $l=0$ ) component (dotted-line curve); the  $p$  ( $l=1$ ) component (full-line curve).

is very similar to that of the total DOS. The higher angular momentum components at the H sites are vanishingly small for the two low-lying bands. In contrast, the contribution of these states at the metal site is important, particularly, the  $d$  ( $l=2$ ) contribution is the major component at the metal site. Its amplitude remains, however, always a factor of 3 smaller than the hydrogen  $s$  states' contribution. Figure 7 shows the presence of the metal  $s$  states at the low-energy side of the first two bands while the metal  $p$  states give an important

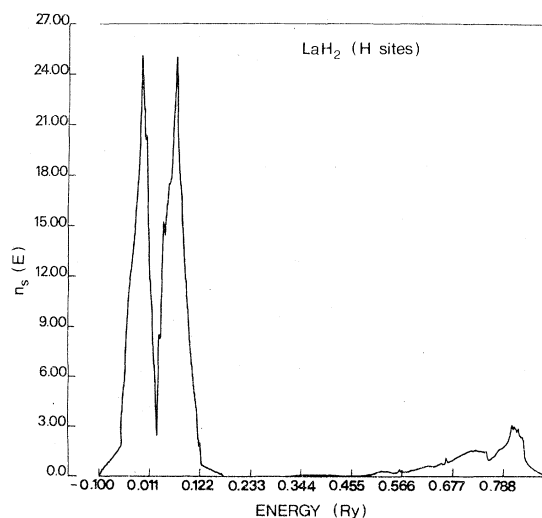


FIG. 8. Partial  $s$  ( $l=0$ ) DOS inside the muffin-tin spheres of the two hydrogen atoms. Units are states of both spin/Ry unit cell.

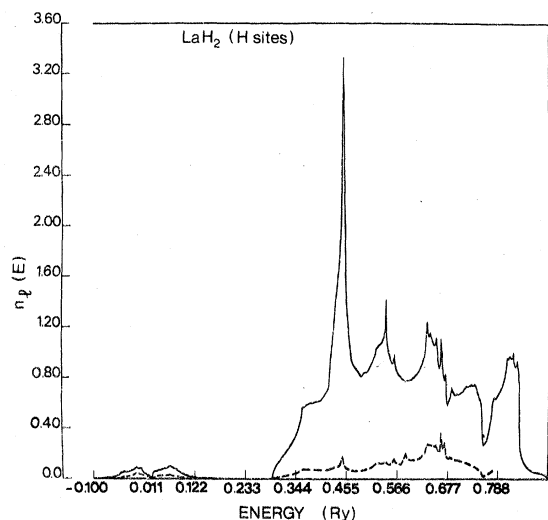


FIG. 9. Partial-wave analysis of the DOS inside the muffin-tin spheres of the two hydrogen atoms. Units are states of both spin/Ry unit cell. The  $p$  ( $l=1$ ) component (full-line curve); the  $d$  ( $l=2$ ) component (dashed-line curve).

contribution to the second peak observed in the DOS.

Above the energy gap, Figs. 6–9 show that the bands are formed essentially of metal  $d$  states. This is not to say that these bands are identical to the pure rare-earth-metal  $d$  bands since, as we emphasized previously, some metal  $d$ , and to a lesser extent, some metal  $s$  and  $p$  states have been considerably affected by the metal-hydrogen interaction and are found at lower energies. We have shown that the hybridization is important in the low-lying bands which should not be considered as formed uniquely of hydrogen states; thus the dihydride cannot be considered literally as an ionic compound. However, the position of the Fermi level and the depopulation of the metal  $d$  bands explain the relative success of some aspects of the anionic model. We wish in this connection to recall here that for the magnetic rare-earth hydrides, the temperature dependence of the magnetic susceptibility,<sup>30</sup> the analysis of Mössbauer data,<sup>34</sup> and the interpretation of the neutron scattering experiments<sup>35</sup> in terms of the magnetic moment of the rare-earth ions are only compatible with a splitting pattern of the energy levels of the  $L$  ions in a cubic environment of H<sup>-</sup> ions.

Photoelectron spectroscopy (PES) and x-ray emission data provide the direct means of studying the total and angular momentum components of the DOS for the valence- and conduction-band states. In the case of hydrides, these data give precious information concerning the position of the hydrogen-derived states. The first uv photoemission

data were obtained for the Pd-H (Ref. 36) and Ti-H systems,<sup>37</sup> and the peaks observed, respectively, at 5.4 and 5 eV below the Fermi energy were attributed to metal-hydrogen bonding states. The composition of the samples was, however, not well defined in these experiments. The photoemission spectra of thorium hydrides<sup>38</sup> also revealed the existence of hydrogen-derived states at low energy. Other transition- and rare-earth-metal hydrides have recently been investigated by ultraviolet photoemission spectroscopy (UPS) (Ref. 16) and by optical studies.<sup>39</sup> Soft x-ray emission spectroscopy on V-H systems<sup>40</sup> also show the presence of hydrogen- $1s$ -vanadium- $3d$  states at 7 eV below  $E_F$ . Similarly in the x-ray photoemission spectroscopy (XPS) measurements<sup>41</sup> on ZrH<sub>1.65</sub>, a strong peak associated with hydrogen  $s$  electrons appeared at 7 eV below  $E_F$ .

If we assume the matrix elements of the photoionization cross sections to be constant and ignore their angular momentum dependence, the total DOS of LaH<sub>2</sub> shown in Fig. 2 can be compared with photoelectron-energy distribution curves.<sup>16</sup> The calculated  $d$ -band width of 1.44 eV with the presence of a shoulder in the DOS starting at 0.76 eV below  $E_F$ , which has been assigned to flat bands around  $K_1$  and  $W'_2$ , as well as the position of the metal-hydrogen-derived bands centered at 4.9 eV below  $E_F$  shows good agreement with the recent, as yet unpublished, data of Weaver and Peterman<sup>16</sup> since the experimental  $d$ -band width is 1.5 eV and the bonding metal-hydrogen bands are centered at 4.7 eV below  $E_F$ . The DOS of LaH<sub>2</sub> obtained in the present work, and previously reported calculation<sup>4</sup> on ErH<sub>2</sub> show the same general features. In ErH<sub>2</sub>, the metal  $d$  bands of width 1.78 eV also presented a shoulder starting at 1 eV below  $E_F$  which could be assigned to the same flat bands as previously noted for LaH<sub>2</sub>. The low-lying metal-hydrogen hybridized bands of ErH<sub>2</sub> centered at 5.5 eV below  $E_F$  also have the two-peak structure mentioned for LaH<sub>2</sub>. An additional shoulder at 6.89 eV below  $E_F$  is present in the DOS of ErH<sub>2</sub> which originates from the lowest  $L_1$  point in the band structure. This shoulder merges with the first peak in the case of LaH<sub>2</sub>. The difference in the position of the low-lying bands or in the value of the gap separating them from the metal  $d$  bands can be traced back essentially to the lattice contraction observed from LaH<sub>2</sub> to ErH<sub>2</sub>; nevertheless, the salient features of the band structure which appear in the DOS remain remarkably similar across the  $L$  row.

Sarma and Bos<sup>15</sup> studied the  $L_{III}$  x-ray emission edge of La in several compounds including hydrides with the LaH<sub>2.18</sub>, LaH<sub>2.45</sub>, and LaH<sub>2.88</sub> compositions. They observed a decrease in the intensity of the emission edge of La upon increasing hydrogenation.



The similarity of the emission edge of  $\text{LaH}_{2.88}$  to those of  $\text{La}_2\text{O}_3$  and  $\text{LaF}_3$  led these authors to interpret their data in terms of the anionic model. The observed depopulation of the  $d$  bands with increasing hydrogen content is in agreement with the present calculation.

In order to characterize more completely the states at the Fermi level, we give in Table II a site and angular momentum analysis of the DOS at  $E_F$ . In spite of the decrease in the metal  $d$  DOS from La to  $\text{LaH}_2$ , this component remains the largest one at  $E_F$ . A non-negligible metal  $p$  contribution is also obtained while the metal  $s$  states usually present at the bottom of a transition- or rare-earth-metal conduction band are found at lower energies in the metal-hydrogen bonding bands. The metal states largely dominate at  $E_F$  the hydrogen states' contribution, a feature common to all the trivalent rare-earth and transition-metal dihydrides. We shall see in the next section the consequences of this feature on the value of the electron-phonon interaction.

#### V. ELECTRON-PHONON INTERACTION IN $\text{LaH}_2$

Since the discovery of superconductivity in  $\text{Th}_3\text{H}_{15}$  (Ref. 42) and in the Pd-H systems,<sup>43</sup> other metal hydrides have been considered as possible candidates. The pure La metal is known to be a superconductor<sup>44</sup> with quite high superconducting transition temperature  $T_c$  rising dramatically with pressure ( $T_c = 4.9$  K and 6 K at normal pressure, respectively, for the  $d$ -hcp and the fcc phases). We addressed ourselves to the question of finding whether the electronic properties of  $\text{LaH}_2$  indicate the possibility of a strong electron-phonon coupling in this material. We will not consider here the possible role of  $f$  levels in promoting or adversely affecting superconductivity; the bands of  $\text{LaH}_2$  near the Fermi energy will instead be treated like transition-metal bands.

In this study of the transition metals, McMillan<sup>45</sup> related  $T_c$  to the electron-phonon mass enhancement  $\lambda$  which he expressed in terms of the ratio of an electronic contribution  $\eta$  to a phonon contribution in the following way:

$$\lambda = \frac{N_f(E_F)\langle I^2 \rangle}{M\langle \omega^2 \rangle} = \frac{\eta}{M\langle \omega^2 \rangle}, \quad (1)$$

where  $N_f(E_F)$  is the DOS at  $E_F$  per spin,  $\langle I^2 \rangle$  is the FS average of the square of the electron-phonon matrix element, and  $\langle \omega^2 \rangle$  is a mean-square phonon frequency defined in Ref. 45.  $M\langle \omega^2 \rangle$  can thus be considered as a phonon force constant, suitably averaged.

Following the idea of Hopfield<sup>46</sup> who first used the angular momentum representation of the Bloch

TABLE II. The partial-wave analysis  $n_l$  of the DOS inside the muffin-tin La and two H spheres at the Fermi energy  $E_F$ . Units are states of both spin/Ry unit cell. The total DOS at  $E_F$  is  $N(E_F) = 15.05$  states of both spin/Ry unit cell.

	La sphere	2H spheres
$n_s$ ( $l=0$ )	0.034	0.068
$n_p$ ( $l=1$ )	0.336	0.616
$n_d$ ( $l=2$ )	6.500	0.067

wave functions to calculate  $\langle I^2 \rangle$ , Gaspari and Gyorffy<sup>17</sup> derived a convenient expression for  $\langle I^2 \rangle$  which is based upon the rigid-ion approximation and involves quantities which can be obtained from ab initio band-structure calculations; namely, they obtained

$$\langle I^2 \rangle = \sum_K \frac{E_F}{\pi^2} \sum_l 2(l+1) \sin^2(\delta_{l+1}^K - \delta_l^K) \times \frac{n_l^K(E_F)n_{l+1}^K(E_F)}{n_{l+1}^{K(1)}(E_F)n_l^{K(1)}(E_F)}. \quad (2)$$

In this expression, the summation on  $K$  runs on all the atoms in the unit cell,  $\delta_l^K$  is the phase shift at the Fermi energy of the scattering muffin-tin (MT) potential of the  $K$  site,  $n_l^K(E_F)$  is the partial DOS at  $E_F$  for site  $K$  with angular momentum  $l$  and  $n_l^{K(1)}(E_F)$  is the corresponding partial DOS of a free scatterer. Calculations of  $\lambda$  using this model have been now performed for a number of transition metals and compounds and particularly for the Pd-H system.<sup>47</sup> For compounds like  $\text{LaH}_2$  with large mass difference between the constituents,  $\lambda$  is often approximated by

$$\lambda_{\text{LaH}_2} \simeq \lambda_{\text{La}} + \lambda_{2\text{H}} = \frac{\eta_{\text{La}}}{M_{\text{La}}\langle \omega^2 \rangle_{\text{acoustic}}} + \frac{\eta_{2\text{H}}}{M_{\text{H}}\langle \omega^2 \rangle_{\text{optic}}}. \quad (3)$$

Several of the quantities entering Eq. (2) are listed in Table III. At the hydrogen site, the  $s$ -scattering phase shift is very large and corresponds nearly to a resonance  $\delta_0 = \frac{1}{2}\pi$ . The importance of the magnitude of  $\delta_0$  at the hydrogen site is consistently observed for all the transition-metal hydrides, with of course some light variation with the compound under study. The phase shifts of the higher angular momentum components are very small; thus, at the H site the  $s$ - $p$  scattering gives the major contribution (81%) to the electron-phonon coupling  $\eta_{\text{H}}$ . The value of  $\eta_{\text{H}}$  per hydrogen atom in  $\text{LaH}_2$  is very small since we find  $\eta_{\text{H}} = 0.0436$  eV/Å<sup>2</sup> compared to  $\eta_{\text{H}} = 0.641$  eV/Å<sup>2</sup> for H in PdH. As we can see from Eq. (2), and keeping in mind that in the metal hydrides, the  $s$  phase shift at the H site is always large, the value of  $\eta_{\text{H}}$  depends sensitively upon the

TABLE III. Values of various parameters entering the calculation of  $\lambda$  for LaH<sub>2</sub>. Symbols are defined in Sec. V of the text. Phase shifts  $\delta_i$  are given in radians.

	$\delta_0$	$\delta_1$	$\delta_2$	$\eta$ (eV/Å <sup>2</sup> )	$M\langle\omega^2\rangle$ (eV/Å <sup>2</sup> )	$\lambda$
La site in LaH <sub>2</sub>	-1.1006	-0.4556	0.5326	0.7565	7.35	0.103
H site in LaH <sub>2</sub>	1.5290	0.0400	0.0009	0.0436	3.35	0.013

magnitude of the partial  $s$  and  $p$  densities of states at the Fermi energy which in the case of LaH<sub>2</sub> are very small. So even if the optic modes in LaH<sub>2</sub> were anomalously soft as in superconducting PdH, the contribution of the hydrogen atoms to  $\lambda$  in LaH<sub>2</sub> would remain small since the electronic contribution is an order of magnitude smaller than the PdH. Neutron scattering experiments<sup>48</sup> on LaH<sub>1.96</sub> indicate that the peak position of the optic modes of this compound is located at 103 meV compared to 58 meV in  $\beta$ -PdH<sub>0.7</sub>; thus the hardening of the optic modes will further reduce the value of  $\lambda_H$  in LaH<sub>2</sub>. Unlike in PdH,<sup>49</sup> the electron-optical-phonon coupling is thus expected to give a negligible contribution to  $\lambda$  in LaH<sub>2</sub>. If we examine the contribution to  $\eta$  provided by the metal site we can see in Table III that at the rare-earth site  $\delta_0$  and  $\delta_1$  are negative, which indicates that the potential is repulsive for  $s$  and  $p$  electrons, as it is also the case for transition metals.  $\delta_2$  is positive but small; this is not surprising since the Fermi energy lies at the bottom of the rare-earth  $5d$  bands at an energy well below the resonance in the  $d$ -wave phase shift. At the La site, 60% of the contribution to  $\eta_{La}$  is provided by the  $p$ - $d$  scattering mechanism, while the  $d$ - $f$  mechanism which is the dominant term in the case of transition metals gives only 37% of the total contribution to  $\eta_{La}$ .

In order to give an estimate of  $\lambda$ , we need to evaluate the effective force constants  $M\langle\omega^2\rangle$  which enter the denominators of Eq. (3). At the H site we have used the value obtained from an analysis of the optical phonons of PdH, and scaled this result by the square of the ratio of the peak positions of the optic modes. We obtain for LaH<sub>2</sub>  $M_H\langle\omega^2\rangle_H = 3.35$  eV/Å<sup>2</sup>; this gives a value of  $\lambda_{2H} = 0.026$  for the two hydrogen atoms in LaH<sub>2</sub>. At the La site, we used the approximation value  $M\langle\omega^2\rangle_{La} \approx \frac{1}{2}M_{La}\Theta_D^2$  with the value  $\Theta_D = 243$  K obtained for LaH<sub>2.03</sub> from low-temperature specific-heat measurements.<sup>50</sup> We find  $M_{La}\langle\omega^2\rangle_{La} = 7.35$  eV/Å<sup>2</sup> and

thus  $\lambda_{La} = 0.103$ .

The total value of  $\lambda$  for LaH<sub>2</sub> is thus very small:  $\lambda_{LaH_2} = 0.13$ .  $T_c$  can then be calculated from the original BCS expression<sup>51</sup>:

$$T_c = \frac{\Theta_D}{1.45} \exp\left(-\frac{1}{\lambda - \mu^*}\right). \quad (4)$$

Using  $\mu^* = 0.1$  in Eq. (4) gives  $T_c \approx 0$  K for LaH<sub>2</sub>. Thus LaH<sub>2</sub> according to the present result should not be a superconductor. This result is in agreement with the experimental investigation of Merriam and Schreiber<sup>18</sup> since these authors found that lanthanum hydride samples with hydrogen-to-metal ratios of 1.8, 1.96, 2.03, 2.11, 2.15, and 2.36 are not superconducting at 1.1 K and that LaH<sub>1.96</sub> is not superconducting at 0.33 K.

## VI. CONCLUSION

We wish here to return briefly to some characteristics of the electronic structure of the  $L$  hydrides, in order to avoid the sometimes misleading aspects of pictures which are too schematic. We have shown here that upon increasing hydrogenation, the metal  $5d$  bands of La appear to be depopulated in favor of low-lying bands which result of the metal-hydrogen and hydrogen-hydrogen interactions. This picture which is in agreement with the saline nature of the  $L$  hydrides and explains successfully numerous experiments such as the variation with hydrogen content in the electrical conductivity, the heat capacity, the magnetic susceptibility etc., should however by no means be understood in terms of a rigid shift of the Fermi level applied to the bands of the pure metal. We have shown instead that the metal interaction results in a deformation of the metal  $5d$  bands and that the low-lying bands found in the hydrides are not formed uniquely of hydrogen  $s$  states but rather show a strong hybridization with metal  $d$  and also metal  $s$  and  $p$  states.

\*Address where all correspondence should be sent.

- <sup>1</sup>See, for example, F. A. Lewis, *The Palladium-Hydrogen System* (Academic, New York, 1967); W. M. Mueller, J. P. Blackledge, and G. G. Libowitz, *Metal Hydrides* (Academic, New York, 1968); G. G. Libowitz, *The Solid-State Chemistry of Binary-Metal Hydrides* (Benjamin, New York, 1965), and references therein.
- <sup>2</sup>A. C. Switendick, *Solid State Commun.* **8**, 1463 (1970); *Ber. Bunsenges. Phys. Chem.* **76**, 535 (1978); *J. Less-Common Met.* **49**, 283 (1976).
- <sup>3</sup>A. C. Switendick, *Int. J. Quantum Chem.* **5**, 459 (1971).
- <sup>4</sup>Michèle Gupta, *Solid State Commun.* **27**, 1355 (1978).
- <sup>5</sup>N. I. Kulikov and A. D. Zvonkov, in *The Proceedings of the International Conference on Hydrogen in Metals, Münster, 1979*, edited by E. Wicke and H. Züchner (Akademische Verlagsgesellschaft, Wiesbaden, 1979), p. 479.
- <sup>6</sup>J. N. Daou, *C. R. Acad. Sci.* **250**, 3165 (1960); J. N. Daou, Thèse d'État, Paris, 1962 (unpublished). J. N. Daou and J. Bonnet, *C. R. Acad. Sci.* **261**, 1675 (1975).
- <sup>7</sup>R. C. Heckman, Sandia Corp. Report SC-RR-69-571 (U.S.A.E.C.) Nov. 1969.
- <sup>8</sup>B. Stalinski, *Bull. Acad. Pol. Sci. Cl. 3* **5**, 1001 (1957).
- <sup>9</sup>Z. Bieganski and B. Stalinski, *Phys. Status Solidi A* **2**, K161 (1970); Z. Bieganski and M. Drulis, *Phys. Status Solidi A* **44**, 91 (1977).
- <sup>10</sup>B. Stalinski, *Bull. Acad. Pol. Sci. Cl. 3* **5**, 997 (1957).
- <sup>11</sup>W. E. Wallace and K. H. Mader, *J. Chem. Phys.* **48**, 84 (1968).
- <sup>12</sup>D. S. Schreiber and R. M. Cotts, *Phys. Rev.* **131**, 1118 (1963).
- <sup>13</sup>W. G. Bos and H. S. Gutowsky, *Inorg. Chem.* **6**, 552 (1967).
- <sup>14</sup>H. Barrère, Thèse de Doctorat d'État, Paris, 1970 (unpublished).
- <sup>15</sup>A. C. Sarma and W. G. Bos, *J. Phys. Chem. Solids* **32**, 1423 (1971).
- <sup>16</sup>J. H. Weaver, *Bull. Am. Phys. Soc.* **23**, 295 (1978); and private communication.
- <sup>17</sup>G. D. Gaspari and B. L. Gyorffy, *Phys. Rev. Lett.* **29**, 801 (1972).
- <sup>18</sup>M. F. Merriam and D. S. Schreiber, *J. Phys. Chem. Solids* **24**, 1375 (1963).
- <sup>19</sup>Michèle Gupta, *Solid State Commun.* **29**, 47 (1979).
- <sup>20</sup>J. C. Slater, *Phys. Rev.* **51**, 846 (1937); T. L. Loucks, *The Augmented-Plane-Wave Method* (Benjamin, New York, 1967).
- <sup>21</sup>S. C. Keeton and T. L. Loucks, *Phys. Rev.* **168**, 672 (1968).
- <sup>22</sup>G. Lehman and M. Taut, *Phys. Status Solidi* **37**, K27 (1970).
- <sup>23</sup>F. Ducastelle, R. Caudron, and P. Costa, *J. Phys.* **31**, 57 (1970).
- <sup>24</sup>D. J. Peterman, B. N. Harmon, J. Marchiando, and J. H. Weaver, *Phys. Rev. B* **19**, 4867 (1979).
- <sup>25</sup>G. G. Libowitz, *Ber. Bunsenges. Phys. Chem.* **76**, 837 (1972).
- <sup>26</sup>G. S. Fleming, S. H. Liu, and T. L. Loucks, *Phys. Rev. Lett.* **21**, 1524 (1968).
- <sup>27</sup>D. L. Johnson and D. K. Finnemore, *Phys. Rev.* **158**, 376 (1967).
- <sup>28</sup>D. S. Schreiber, *Phys. Rev.* **137**, A860 (1965).
- <sup>29</sup>See the review article by T. Kasuya, in *Magnetism*, edited by G. T. Rado and H. Suhl (Academic, New York, 1966), Vol. II B, pp. 215-294.
- <sup>30</sup>W. E. Wallace, *Ber. Bunsenges. Phys. Chem.* **76**, 832 (1972).
- <sup>31</sup>R. S. Kashaev, A. N. Gil'manov, F. F. Gubaibullin, and M. E. Kost, *Fiz. Tverd. Tela* **20**, 3 (1978) [*Sov. Phys.—Solid State* **20**, 1 (1978)].
- <sup>32</sup>R. C. Heckman, *J. Chem. Phys.* **46**, 2158 (1967); **48**, 5281 (1968).
- <sup>33</sup>W. G. Bos, *J. Chem. Phys.* **53**, 855 (1970).
- <sup>34</sup>G. K. Shenoy, B. D. Dunlap, D. G. Westlake, and A. E. Dwight, *Phys. Rev. B* **14**, 41 (1976).
- <sup>35</sup>H. Shaked, J. Faber, M. H. Mueller, and D. G. Westlake, *Phys. Rev. B* **16**, 340 (1977).
- <sup>36</sup>D. E. Eastman, J. K. Cashion, and A. C. Switendick, *Phys. Rev. Lett.* **27**, 35 (1971).
- <sup>37</sup>D. E. Eastman, *Solid State Commun.* **10**, 933 (1972).
- <sup>38</sup>J. H. Weaver, J. A. Knapp, D. E. Eastman, D. T. Peterson, and C. B. Satterthwaite, *Phys. Rev. Lett.* **39**, 639 (1977).
- <sup>39</sup>J. H. Weaver, R. Rosei, and D. T. Peterson, *Phys. Rev. B* **19**, 4855 (1979).
- <sup>40</sup>Y. Fukai, S. Kazama, T. Tanaka, and M. Matsumoto, *Solid State Commun.* **19**, 507 (1976).
- <sup>41</sup>B. W. Veal, D. J. Lam, and D. G. Westlake, *Phys. Rev. B* **19**, 2856 (1979).
- <sup>42</sup>C. B. Satterthwaite and I. L. Toepke, *Phys. Rev. Lett.* **25**, 741 (1970).
- <sup>43</sup>T. Skoskiewicz, *Phys. Status Solidi A* **11**, K 123 (1972); B. Strizker and W. Buckel, *J. Phys.* **257**, 1 (1972).
- <sup>44</sup>M. B. Maple, J. Wittig, and K. S. Kim, *Phys. Rev. Lett.* **23**, 1375 (1969).
- <sup>45</sup>W. L. McMillan, *Phys. Rev.* **167**, 331 (1968).
- <sup>46</sup>J. J. Hopfield, *Phys. Rev.* **186**, 443 (1969).
- <sup>47</sup>D. A. Papaconstantopoulos and B. M. Klein, *Phys. Rev. Lett.* **35**, 110 (1975); D. A. Papaconstantopoulos, B. M. Klein, J. S. Faulkner, and L. L. Boyer, *Phys. Rev. B* **18**, 2784 (1978).
- <sup>48</sup>D. G. Hunt and D. K. Ross, *J. Less-Common Met.* **49**, 169 (1976).
- <sup>49</sup>J. P. Burger and D. S. McLachlan, *J. Phys. (Paris)* **37**, 1227 (1976); J. P. Burger, S. Senoussi, and B. Souffaché, *J. Less-Common Met.* **49**, 213 (1976).
- <sup>50</sup>Z. Bieganski, D. Gonzalez-Alvarez, and F. W. Klaayzen, *Physica* **37**, 153 (1967).
- <sup>51</sup>J. Bardeen, L. N. Cooper, and J. R. Schrieffer, *Phys. Rev.* **106**, 162 (1957); **108**, 1175 (1957).